Desalination and Water Treatment
www.deswater.com

doi: 10.5004/dwt.2022.28856

272 (2022) 138–143
October

Efficient catalytic reduction of 4-nitrophenol by magnetic Cu/Fe nanocomposite catalyst

Qiang Li[a,b,*], Huo Zhou[a], Guangyong Li[a], Yuxuan Ye[a,b], Dongsheng Xia[a,b,*]

[a]*School of Environmental Engineering, Wuhan Textile University, Wuhan 430073, China, Tel. +86-27-59367338; emails: qiangli@wtu.edu.cn (Q. Li), dongsheng_xia@wtu.edu.cn (D.S. Xia), zhou7742@outlook.com (H. Zhou), 3160663995@qq.com (G.Y. Li), yxye@wtu.edu.cn (Y. Ye)*
[b]*Engineering Research Center for Clean Production of Textile Dyeing and Printing, Ministry of Education, Wuhan 430073, China*

Received 30 April 2022; Accepted 17 August 2022

ABSTRACT

This study reported the preparation of the magnetic Cu/Fe nanocomposite catalyst by co-precipitation method and its catalytic performance was examined for the reduction of 4-nitrophenol (4-NP). The catalyst was characterized by X-ray diffraction, scanning electron microscopy, transmission electron microscopy, and vibrating-sample magnetometer. The characterization indicated that the fabricated catalyst was spherical nanoparticles with porous structures and owned good magnetism in the aqueous solution. The nanocomposite of Cu:Fe = 1.5 had higher catalytic performance, and 95% of 4-NP could be catalytically reduced to 4-aminophenol (4-AP) with 15 min at 55°C. The catalytic conversion rate can reach 80% in the 4th cycle. The catalytic performance of consecutive cycles showed high activity and stability of the catalyst. All the results indicate that the magnetic Fe/Cu nanocomposite catalyst is a promising catalyst in the reduction of 4-nitrophenol.

Keywords: Magnetic Fe/Cu nanocomposite; Reduction; 4-nitrophenol; Catalytic activity

1. Introduction

The 4-nitrophenol (4-NP) is one of the hazardous and toxic pollutants, which widely exist in various untreated industrial effluents [1,2]. Due to its high solubility and toxic, 4-NP in aqueous is hard to be biodegraded and decomposed [3]. Traditional water purification methods for removing 4-NP are not effective [4]. Many researchers have reported that catalytic reduction is recognized as one of the most promising technology for pollutants degradation and removal in mild conditions [5]. 4-NP can be converted to 4-aminophenol (4-AP), which is less poisonous than 4-NP by catalytic reduction method. The catalytic reduction of 4-NP has attracted more and more attention.

The catalytic reduction of 4-NP to 4-AP has been extensively studied in recent years [2,6]. More and more studies have been focused on metal nanoparticle catalysts, such as Au [7], Pt [8], Ag [9], and Pb [10]. These metal catalysts own high activity in the catalytic reduction of 4-NP, but they are too expensive. Many studies suggest that copper-based catalyst is a good replacement in terms of its low cost and material abundance. Copper-based catalyst has been employed in the reduction of 4-NP recently [2,11–16]. Their catalytic performance has been studied extensively in the reactions of industrial and environmental applications. However, one major question associated with copper-based nanoparticle catalysts is the property of poor separation in the reaction. In order to solve the problem, much attention has been focused on the development of new supporting materials for introducing magnetic particles [17]. The magnetic composite catalyst also exhibits high stability, dispersion and catalytic efficiency. Many studies

* Corresponding authors.

on different kinds of supporting magnetic materials for the catalytic reaction have appeared. Feng et al. [18] reported that $CuFe_2O_4$ magnetic nanoparticles owned high catalytic activity in the reduction of 4-NP, but its catalytic performance was decreased in the second catalytic cycle. Dey et al. [19] synthesized copper ferrite magnetic nanoparticles for catalytic reduction for 4-NP, it is easily separable by an external magnetic field from the solution. Ghorbani-Vaghei et al. [20] reported the synthesis of Au nanoparticles (Au NPs) fabricated alginate immobilized cubic shaped magnetite (Fe_3O_4@Alg-Au NPs). The core-shell like Fe_3O_4@Alg composite acted as a suitable stabilizer for the anchored Au NPs. It exhibited high rate constant in the reduction of 4-NP. Filiz [21] reported the nature of the interactions between Cu oxide particles and metal oxides was one of the primary interests to successfully design new catalyst with improved activity for the 4-NP reduction. Nasrollahzadeh et al. [22] studied the synthesis of the Cu/Fe_3O_4 nanoparticles using *Morinda morindoides* leaf aqueous extract and it exhibited remarkable and durable activity for the reduction of 4-NP. Sajjadi et al. [23] reported magnetic nanoparticles supported N-heterocyclic palladium(II) nanocatalyst based on surface Fe_3O_4. The application of Fe_3O_4@SiO_2-Thiotet-Pd(II) for the reduction of 4-NP indicated highly active and magnetically recyclable [23]. However, limited knowledge had been reported on the interactions between Cu oxide particles and iron oxides for catalytic reduction of 4-NP. The characteristics and catalytic activities of Cu oxide particles loading capacity are not known.

So, based on the above-mentioned examples, the present study proposed the construction of a magnetic catalyst for catalytic reduction of 4-NP to 4-AP. The effect molar ratio of Cu/Fe, as well as various amounts of catalyst, $NaBH_4$ dosage, 4-NP concentration, and temperature on the catalytic reduction reaction, were discussed. The kinetic analysis and reaction activation energy of the reaction system were also conducted to explore the catalytic reduction performance of the catalyst. The catalytic efficiency and stability of the magnetic Fe/Cu composite catalyst were verified by the recycling experiment.

2. Experimental

2.1. Materials

4-nitrophenol (4-NP, 99%), sodium borohydride ($NaBH_4$, 99%), ferric nitrate nonahydrate ($Fe(NO_3)_3{\cdot}9H_2O$, 99%), copper nitrate hydrate ($Cu(NO_3)_2{\cdot}3H_2O$, 99%), propylene oxide (C_3H_6O, 99%) and ethanol (C_2H_5OH, 99%) were purchased from Sinopharm Chemical Reagent Co., Ltd. All the chemicals were analytical reagent grade and were used without further purification. Ultrapure water was used for all synthesis and treatment.

2.2. Fabrication magnetic Cu/Fe nanocomposite

1.5 g of $Cu(NO_3)_2{\cdot}3H_2O$ and 5.007 g of $Fe(NO_3)_3{\cdot}9H_2O$ were dissolved in 120 mL ethanol. At 60°C, 15 mL epoxy propane was added and stirred for 15 min to produce a reddish-brown flocculated gel. The gel was aged at room temperature for 24 h. Then the gel was centrifuged and separated. The residual was dried at 60°C. Finally, the catalyst (Cu:Fe = 1.5) was obtained after being calcined at 500°C for 2 h. The different molar ratios of Cu/Fe catalysts (Cu:Fe = 0.5, Cu:Fe = 1.0) were prepared in the same condition.

2.3. Characterizations

The crystal structure and phase purity of the catalyst were analyzed by X-ray diffraction (XRD) using D8 advance X-ray diffraction (Bruker AXS Company, Germany) equipped with Cu Kα radiation (λ = 1.5406 Å). The functional group of the catalyst was characterized by the Fourier-transform infrared spectrum (FTIR, Bruker Vertex 70, Germany). The surface morphology picture of the catalyst was performed on a scanning electron microscope (Sigma HD-SEM, Germany) operated at an acceleration voltage of 10 kV. The magnetic property of the catalyst was analyzed by PPMS-9 (Quantum Design Company, USA).

2.4. Catalytic reduction of 4-NP

The catalytic reduction activity of 4-NP was carried out in a 250 mL flask. The flask was shaken at 150 rpm. The dosage effect of composite catalyst, sodium borohydride, and 4-NP on the reduction efficiency was investigated. In order to obtain the best catalytic performance, the catalytic activities of different molar ratios of Cu/Fe catalysts were measured and compared. The conversion of 4-NP to 4-AP was monitored by a Shimadzu UV 2100 spectrophotometer over a scanning range of 200–500 nm. The reaction rate was measured by the extinction of the solution at 400 nm (absorption of p-nitrophenolate ion) as a function of time.

3. Results and discussion

3.1. Characterization of magnetic Cu/Fe nanocomposite

The structure of the prepared magnetic Cu/Fe nanocomposite catalyst was investigated by XRD. As shown in Fig. 1a, the peaks at 24.13°, 33.12°, 35.60°, 40.82°, 49.41°, 54.00°, 57.51°, and 62.38° were indexed to (012), (104), (110), (113), (024), (116), (018) and (214) planes of Fe_2O_3 (JCPDS PDF#85-0599), respectively, which demonstrated the existence of Fe_2O_3 [24]. The peaks at 2θ = 35.38°, 38.76°, 66.30° and 68.15° can be respectively indexed to (002), (111), (311) and (220) diffractions of CuO (PDF#80-1916), suggesting the formation of CuO particles [25]. The XRD results showed that the synthesized catalyst contained characteristic diffraction peaks of Fe_2O_3 and CuO. Fe and Cu oxides were formed by calcining and aerobic conditions. The FTIR spectra of the fabricated catalyst are shown in Fig. 1b. The suitable peak at 538 cm^{-1} was denoted for the understanding of the metal-oxide bond (Cu–O–Fe). The hysteresis loops vibrating-sample magnetometer (VSM) of magnetic Cu/Fe nanocomposite catalysts with different molar ratios are shown in Fig. 1c. The coercivity of the fabricated catalyst was zero, indicating that it was a typical superparamagnetic catalyst. And the magnetic core was well wrapped in the catalyst, which was conducive to the separation of the catalyst [2]. The magnetization decreased gradually as the increased proportion of copper, which was linked to the

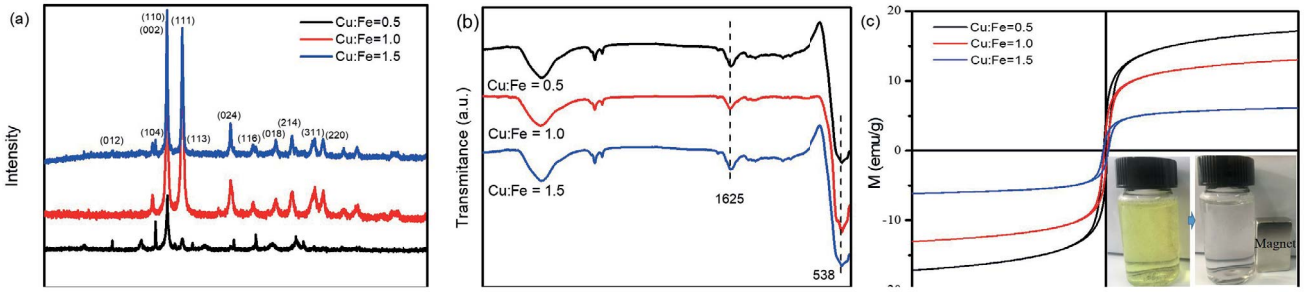

Fig. 1. XRD patterns (a), FTIR spectra (b) and VSM (c) of magnetic Cu/Fe nanocomposite catalysts with the molar ratios of 0.5, 1.0 and 1.5.

decrease in the proportion of iron oxide in the composite catalyst. After the catalytic reaction, the catalyst was completely separated by the magnet from the solution, which indicated that the synthesized catalyst had good magnetism in the aqueous solution.

The SEM images of magnetic Cu/Fe nanocomposite catalysts with the molar ratio of 1.5 are shown in Fig. 2a and b. The results showed that the fabricated catalyst formed homogeneous substances with porous structures. There were many spherical nanoparticles on the surface of the catalyst, which can increase the surface area of the catalyst and the contact frequency between catalyst and reactant.

3.2. Performance under different experimental conditions

After adding the catalyst, the color of the 4-NP solution gradually became colorless. The result indicated that the catalyst owned good catalytic reduction performance. To explore the catalytic properties of different molar ratios of Cu/Fe catalysts, 4-NP was reduced by the composite catalyst and copper oxide. As shown in Fig. 3a, the 4-NP showed no change in the absence of the catalyst. It could be seen that the higher ratio of Cu/Fe in the material, the higher the catalytic efficiency of the catalyst. This was because that copper oxide was the main activity in catalytic reduction of 4-NP [26]. The higher the copper content, the more active sites. The catalytic reduction of 4-NP by copper oxide was lower than that of the composite catalyst (Cu:Fe = 1.5). Iron oxides in composite catalysts can enhance catalytic efficiency.

As shown in Fig. 3b, the absorption peak gradually decreased at 400 nm with the increase of $NaBH_4$ concentration. When the concentration of $NaBH_4$ reached 0.5 g/L, the peak value at 400 nm was close to 0, and the peak value at 300 nm was maximized. The results showed that the catalytic reduction of 4-NP to 4-AP was beneficial with the increase of $NaBH_4$ in a certain concentration range. When the concentration of $NaBH_4$ reached 0.5 g/L, it was enough to provide adequate reductant under this experimental condition. Therefore, the concentration of $NaBH_4$ in the reaction was fixed at 0.5 g/L.

The efficiency of the catalytic reaction is related to the active site of the catalyst. The more catalysts involved in the reaction, the more active sites of the catalyst will naturally be provided. In Fig. 3c, the catalytic efficiency increased with the increase of catalyst dosage. When the dosage of the catalyst reached 50 mg/L, nearly 93% of 4-NP was reduced with the catalyst. The effect of 4-NP initial concentration on the catalytic reduction was also investigated (Fig. 3d). The reduction rate had a little change when the initial concentration of 4-NP was less than 100 mg/L. And it gradually decreased with the increase of the initial concentration of 4-NP. Especially, the sharply decrease phenomenon was discovered when the initial concentration exceeds 100 mg/L. Therefore, 100 mg/L was selected as the substrate concentration in the experiment.

The catalytic efficiency of reducing 4-NP at different temperatures was determined by ultraviolet spectroscopy. The ultraviolet absorption spectrum was taken at intervals within the wavelength range of 200–650 nm. As shown in Fig. 4a–d, the absorption peak gradually decreased at 400 nm. As the temperature increased, the absorption peak at 400 nm decreased faster and faster. For example, the absorption peak values of Fig. 4a–d under 25°C, 35°C, 45°C, 55°C were 0.55, 0.21, 0.17, 0.08 at 15 min, respectively. At 55°C, more than 95% of 4-NP could be catalytically reduced to 4-AP within 15 min. This result was also well received in Fig. 4e. The reaction rate (K) determined from the slope were 0.46×10^{-3} s^{-1}, 0.66×10^{-3} s^{-1}, 1.9×10^{-3} s^{-1}, and 2.6×10^{-3} s^{-1}, respectively. With the increase of temperature, the catalytic efficiency was improved and the time needed to complete the degradation was reduced.

According to Fig. 4e, $\ln(C_t/C_0)$ and time t were linearly fitted at each temperature to calculate the reaction rate (k) at each temperature, and then the Arrhenius behavior of 4-NP degradation was studied in the reaction system. According to Fig. 4f, the catalytic reduction followed Arrhenius behavior well, and the correlation coefficient was about 0.93. According to the Arrhenius equation [27,28], the activation energy (E_a) was 88.87 kJ/mol, which was very low in the related studies.

3.3. Reusability of the catalyst

The reusability of the catalysts is of great significance to the practical application of catalysts. It can be seen from Fig. 5a that the reduction reaction reacted fast in the process. The catalytic conversion rate still reached 80% in the 4th cycle and its conversion rate can maintain 70% in the 5th cycle. The FTIR spectra analysis of the composite catalyst (Cu:Fe = 1.5) after the 5th cycle is shown in Fig. 5b. The results illustrated that the chemical composition of the

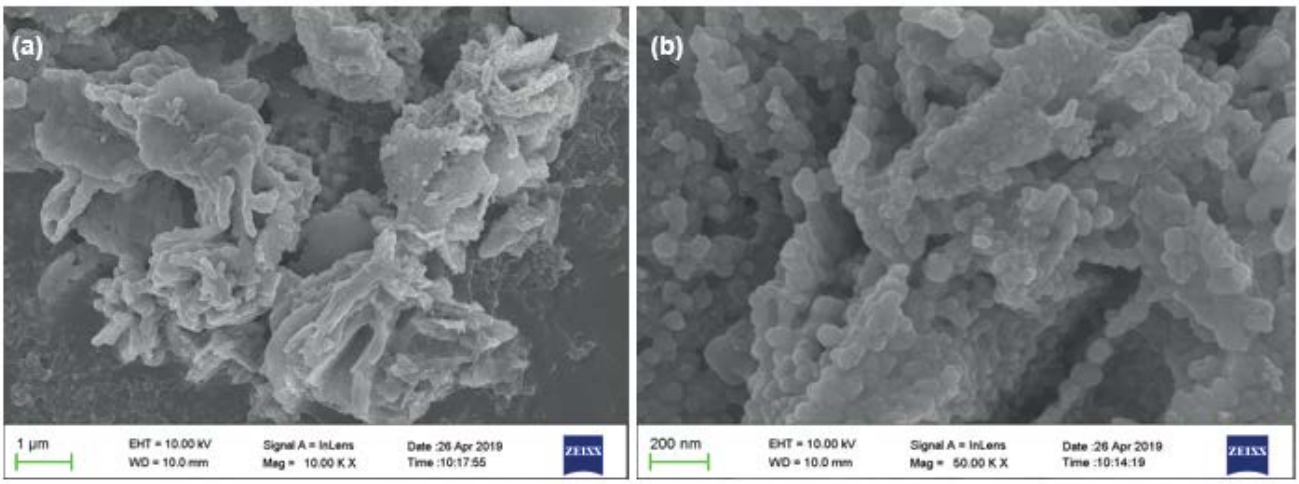

Fig. 2. SEM images of magnetic Cu/Fe nanocomposite catalysts with the molar ratio of 1.5.

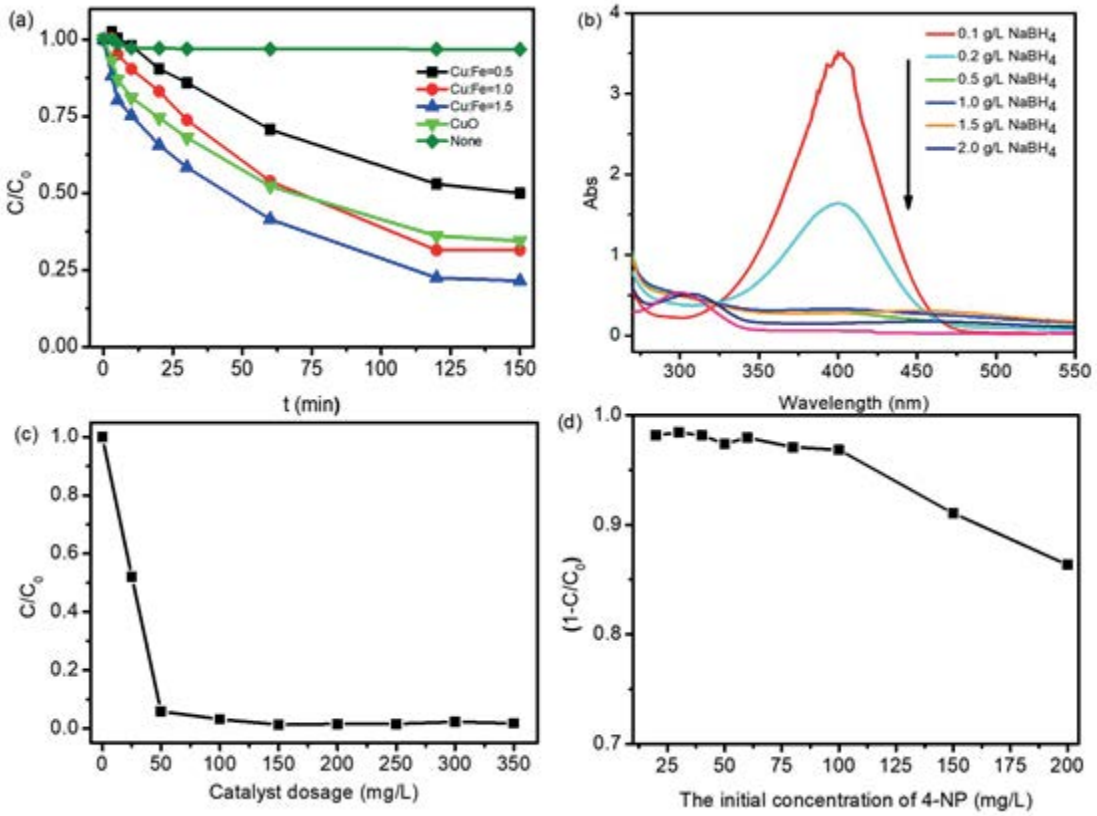

Fig. 3. Effect of different molar ratios of Cu/Fe (a), $NaBH_4$ dosage (b), catalyst dosage (c), the initial concentration of 4-NP on the catalysis reduction (d) (Reaction condition: [4-NP] = 0.03 g/L, [$NaBH_4$] = 0.5 g/L, T = 25°C, without pH adjustment).

recycled catalyst almost remained unaltered. The catalyze performance of five consecutive cycles showed high stability and reusability of the catalyst.

4. Conclusions

We prepared a high efficient and stable magnetic Fe/Cu nanocomposite catalyst for the reduction of 4-NP to 4-AP. Three kinds of Cu/Fe composite catalysts with different Cu/Fe proportions were successfully prepared by co-precipitation. The characterization indicated the fabricated catalyst was spherical nanoparticles with porous structures and owned good magnetism in the aqueous solution. The composite catalyst of Cu:Fe = 1.5 had higher catalytic performance than other Cu/Fe composite catalysts. At 55°C, more than 95% of 4-NP could be catalytically

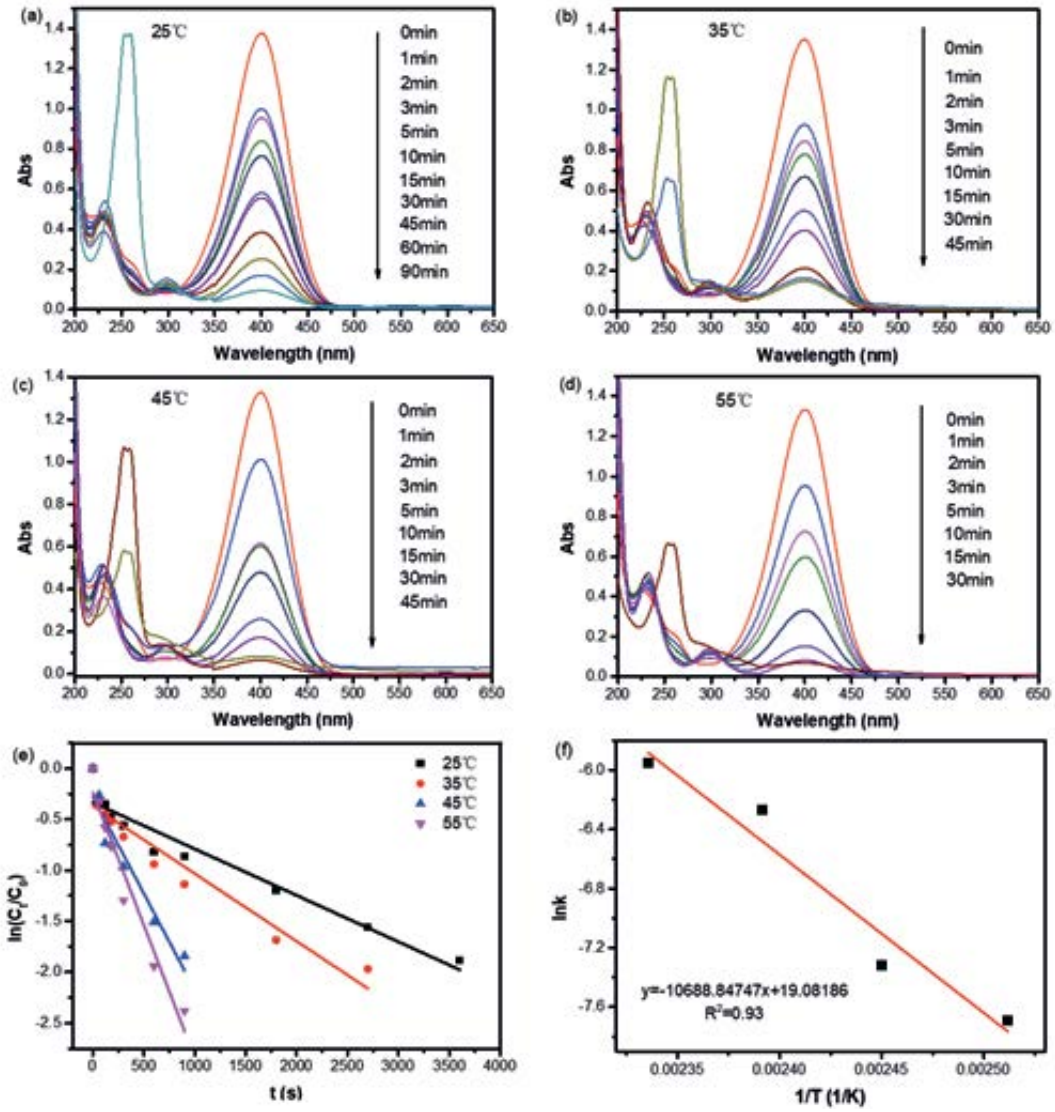

Fig. 4. Catalytic reduction of 4-NP at (a) 25°C, (b) 35°C, (c) 45°C and (d) 55°C was shown by UV-Vis spectra, (e) dynamics experiments at different temperatures, (f) plots of $\ln(C_t/C_0)$ vs. time for the reduction of 4-NP (Reaction condition: ([4-NP] = 0.03 g/L, $[NaBH_4]$ = 0.5 g/L, T = 25°C, without pH adjustment).

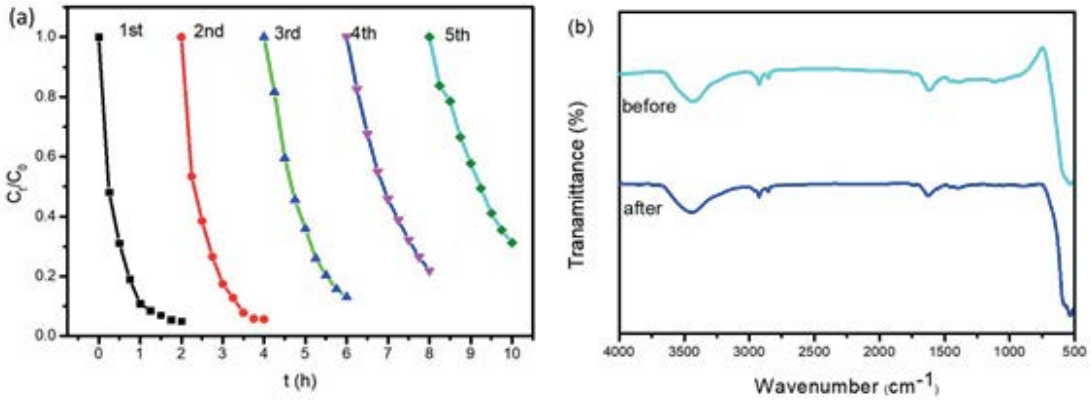

Fig. 5. Reusability of the catalyst for five successive cycles of reactions of 4-NP reduction (a); the FTIR spectra of the catalyst before and after the 5th cycle (b).

reduced to 4-AP within 15 min. The activation energy (E_a) of the reaction was 88.87 KJ/mol. The catalytic performance of consecutive cycles showed high stability and reusability. All the result makes magnetic Fe/Cu nanocomposite catalyst an efficient catalyst in the reduction of 4-nitrophenol.

Acknowledgments

We gratefully acknowledge the generous support provided by the "National Natural Science Foundation of China (51908432)", and the "Natural Science Foundation of Hubei Province (2018CFB397)," China. The authors would like to thank Shiyanjia Lab (www.shiyanjia.com) for the XPS analysis.

Data availability statement

All data, models, and code generated or used during the study appear in the submitted article.

Conflict of interest statement

On behalf of all authors, the corresponding author states that there is no conflict of interest.

References

[1] S. Hu, Y. Guan, W. Yun, H. Han, Nano-magnetic catalyst KF/CaO-Fe_3O_4 for biodiesel production, Appl. Energy, 88 (2011) 2685–2690.
[2] Q. Li, H. Song, Y. Ye, F. Pan, D. Zhang, D. Xia, A green designed copper-resin composite for highly efficient catalytic reduction of 4-nitrophenol, Colloid Interface Sci. Commun., 42 (2021) 100407, doi: 10.1016/j.colcom.2021.100407.
[3] P.S. Silva, B.C. Gasparini, H.A. Magosso, A. Spinell, Gold nanoparticles hosted in a water-soluble silsesquioxane polymer applied as a catalytic material onto an electrochemical sensor for detection of nitrophenol isomers, J. Hazard. Mater., 273 (2014) 70–77.
[4] J. Li, C. Liu, Y. Liu, Au/graphene hydrogel: synthesis, characterization and its use for catalytic reduction of 4-nitrophenol, J. Mater. Chem., 22 (2012) 8426–8430.
[5] M. Guo, J. He, Y. Li, S. Ma, X. Sun, One-step synthesis of hollow porous gold nanoparticles with tunable particle size for the reduction of 4-nitrophenol, J. Hazard. Mater., 310 (2016) 89–97.
[6] S. Gao, Z. Zhang, K. Liu, B. Dong, Direct evidence of plasmonic enhancement on catalytic reduction of 4-nitrophenol over silver nanoparticles supported on flexible fibrous networks, Appl. Catal., B, 188 (2016) 245–252.
[7] D. Berillo, Gold nanoparticles incorporated into cryogel walls for efficient nitrophenol conversion, J. Cleaner Prod., 247 (2019)119089, doi: 10.1016/j.jclepro.2019.119089.
[8] T. Yu, J. Zeng, B. Lim, Y. Xia, Aqueous-phase synthesis of Pt/CeO_2 hybrid nanostructures and their catalytic properties, Adv. Mater., 22 (2010) 5188–5192.
[9] M.M. Ayad, W.A. Amer, S. Zaghlol, N. Maráková, J. Stejskal, Polypyrrole-coated cotton fabric decorated with silver nanoparticles for the catalytic removal of p-nitrophenol from water, Cellulose, 25 (2018) 7393–7407.
[10] J. Zhu, X. Zhang, Z. Qin, L. Zhang, Y. Ye, M. Cao, L. Gao, T. Jiao, Preparation of PdNPs doped chitosan-based composite hydrogels as highly efficient catalysts for reduction of 4-nitrophenol, Colloids Surf., A, 611 (2020) 125889, doi: 10.1016/j.colsurfa.2020.125889.
[11] M. Nasrollahzadeh, S.M. Sajadi, A. Rostami-Vartooni, M. Bagherzadeh, R. Safari, Immobilization of copper nanoparticles on perlite: green synthesis, characterization and catalytic activity on aqueous reduction of 4-nitrophenol, J. Mol. Catal. A: Chem., 400 (2015) 22–30.
[12] L. Hang, Y. Zhao, H. Zhang, G. Liu, L. Qu, Copper nanoparticle@graphene composite arrays and their enhanced catalytic performance, Acta Mater., 105 (2016) 59–67.
[13] L. Jin, G. He, J. Xue, T. Xu, H. Chen, Cu/graphene with high catalytic activity prepared by glucose blowing for reduction of p-nitrophenol, J. Cleaner Prod., 161 (2017) 655–662.
[14] S.B. Khan, F. Ali, K. Akhtar, Chitosan nanocomposite fibers supported copper nanoparticles based perceptive sensor and active catalyst for nitrophenol in real water, Carbohydr. Polym., 207 (2019) 650–662.
[15] X.J. Bai, D. Chen, Y.N. Li, X.M. Yang, M.Y. Zhang, T.Q. Wang, X.M. Zhang, L.Y. Zhang, Y. Fu, X. Qi, W. Qi, Two-dimensional MOF-derived nanoporous Cu/Cu_2O networks as catalytic membrane reactor for the continuous reduction of p-nitrophenol, J. Membr. Sci., 582 (2019) 30–36.
[16] Y. Feng, T. Jiao, J. Yin, L. Zhang, L. Zhang, J. Zhou, Q. Peng, Facile preparation of carbon nanotube-Cu_2O nanocomposites as new catalyst materials for reduction of p-nitrophenol, Nanoscale Res. Lett., 14 (2019) 78, doi: 10.1186/s11671-019-2914-1.
[17] D. Raghunath, S. Venkata Satyanarayana, P. Hugues Kamdem, B. Madhumita, M. Vinesh. M. Arjun, Silver decorated magnetic nanocomposite (Fe_3O_4@PPy-MAA/Ag) as highly active catalyst towards reduction of 4-nitrophenol and toxic organic dyes, Appl. Catal., B, 244 (2019) 546–558.
[18] F. Jie, L. Su, Y. Ma, C. Ren, Q. Guo, X. Chen, J. Feng, L. Su, Y. Ma, C. Ren, $CuFe_2O_4$ magnetic nanoparticles: a simple and efficient catalyst for the reduction of nitrophenol, Chem. Eng. J., 221 (2013) 16–24.
[19] C. Dey, D. De, M. Nandi, M. Goswami, A high performance recyclable magnetic $CuFe_2O_4$ nanocatalyst for facile reduction of 4-nitrophenol, Mater. Chem. Phys., 242 (2020) 122237, doi: 10.1016/j.matchemphys.2019.122237.
[20] R. Ghorbani-Vaghei, H. Veisi, M.H. Aliani, P. Mohammadi, B. Karmakar, Alginate modified magnetic nanoparticles to immobilization of gold nanoparticles as an efficient magnetic nanocatalyst for reduction of 4-nitrophenol in water, J. Mol. Liq., 327 (2020) 114868, doi: 10.1016/j.molliq.2020.114868.
[21] B.C. Filiz, The role of catalyst support on activity of copper oxide nanoparticles for reduction of 4-nitrophenol, Adv. Powder Technol., 31(2020) 3845–3859.
[22] M. Nasrollahzadeh, M. Atarod, S.M. Sajadi, Green synthesis of the Cu/Fe_3O_4 nanoparticles using *Morinda morindoides* leaf aqueous extract: a highly efficient magnetically separable catalyst for the reduction of organic dyes in aqueous medium at room temperature, Appl. Surf. Sci., 364 (2016) 636–644.
[23] M. Sajjadi, M. Nasrollahzadeh, M.R. Tahsili, Catalytic and antimicrobial activities of magnetic nanoparticles supported N-heterocyclic palladium(II) complex: a magnetically recyclable catalyst for the treatment of environmental contaminants in aqueous media, Sep. Purif. Technol., 227 (2019) 115716, doi: 10.1016/j.seppur.2019.115716.
[24] L. Yang, C.S. Chen, Y.J. Tu, Y.H. Huang, Z. Hui, Heterogeneous degradation of organic pollutants by persulfate activated by CuO-Fe_3O_4: mechanism, stability, and effects of pH and bicarbonate ions, Environ. Sci. Technol., 49 (2015) 6838–6845.
[25] W. Li, B. Liu, Y. Wu, Y. Gao, S. Xing, Removal of ciprofloxacin by persulfate activation with CuO: a pH-dependent mechanism, Chem. Eng. J., 382 (2019) 122837, doi: 10.1016/j.cej.2019.122837.
[26] M.V. Morales, M. Rocha, C. Freire, E. Asedegbega-Nieto, E. Gallegos-Suarez, I. Rodríguez-Ramos, A. Guerrero-Ruiz, Development of highly efficient Cu versus Pd catalysts supported on graphitic carbon materials for the reduction of 4-nitrophenol to 4-aminophenol at room temperature, Carbon, 111 (2017) 150–161.
[27] Q. Li, W. Tao, A. Li, Q. Zhou, C. Shuang, Poly(4-vinylpyridine) catalyzed isomerization of maleic acid to fumaric acid, Appl. Catal., A, 484 (2014) 148–153.
[28] T. Wi-Afedzi, F.Y. Yeoh, M.T. Yang, A. Yip, L. Andrew, A comparative study of hexacyanoferrate-based Prussian blue analogue nanocrystals for catalytic reduction of 4-nitrophenol to 4-aminophenol, Sep. Purif. Technol., 218 (2019) 138–145.